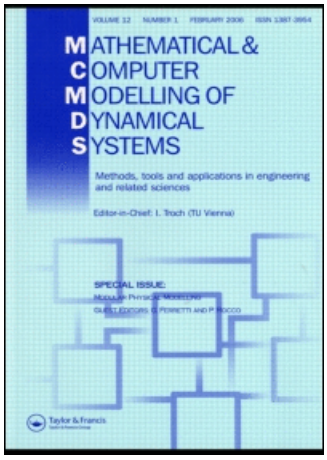

Mathematical and Computer Modelling of Dynamical Systems
Methods, Tools and Applications in Engineering and Related Sciences
Publication details, including instructions for authors and subscription information:
http://www.informaworld.com/smpp/title~content=t713682513

Optimal control of self-organized dynamics in cellular signal transduction

O. Slaby [a]; S. Sager [a]; O. S. Shaik [a]; U. Kummer [b]; D. Lebiedz [a]
[a] Interdisciplinary Center for Scientific Computing, University of Heidelberg, Germany
[b] European Media Laboratory, Heidelberg, Germany

Online Publication Date: 01 October 2007
To cite this Article: Slaby, O., Sager, S., Shaik, O. S., Kummer, U. and Lebiedz, D. (2007) 'Optimal control of self-organized dynamics in cellular signal transduction', Mathematical and Computer Modelling of Dynamical Systems, 13:5, 487 - 502
To link to this article: DOI: 10.1080/13873950701243969
URL: http://dx.doi.org/10.1080/13873950701243969

Mathematical and Computer Modelling of Dynamical Systems
Vol. 13, No. 5, October 2007, 487 – 502

Optimal control of self-organized dynamics in cellular signal transduction

O. SLABY[†], S. SAGER[†], O. S. SHAIK[†], U. KUMMER[‡] and D. LEBIEDZ*[†]

[†]Interdisciplinary Center for Scientific Computing, University of Heidelberg, Germany
[‡]European Media Laboratory, Heidelberg, Germany

We demonstrate how model-based optimal control can be exploited in biological and biochemical modelling applications in several ways. In the first part, we apply optimal control to a detailed kinetic model of a glycolysis oscillator, which plays a central role in immune cells, in order to analyse potential regulatory mechanisms in the dynamics of associated signalling pathways. We demonstrate that the formulation of inverse problems with the aim to determine specific time-dependent input stimuli can provide important insight into dynamic regulations of self-organized cellular signal transduction. In the second part, we present an optimal control study aimed at target-oriented manipulation of a biological rhythm, an internal clock mechanism related to the circadian oscillator. This oscillator is responsible for the approximate endogenous 24 h (latin: circa dies) day-night rhythm in many organisms. On the basis of a kinetic model for the fruit fly Drosophila, we compute switching light stimuli via mixed-integer optimal control that annihilate the oscillations for a fixed time interval. Insight gained from such model-based specific manipulation may be promising in biomedical applications.

Keywords: Self-organization; Biochemical oscillations; Circadian clock; Signal transduction; Inverse problems; Direct multiple shooting; Mixed-integer optimal control; Bang-bang control;

AMS Subject Classifications: 37N25; 49J15; 90C11

1. Introduction

Self-organized dynamical processes under nonequilibrium conditions are often observed as impressing phenomena in nature. Since the elucidation of their theoretical foundations by Glansdorff and Prigogine [1], there is increasing interest in modelling and simulating such phenomena in living systems for a better understanding of the underlying dynamical mechanisms and especially to study their possible physiological significance. Self-organized systems displaying oscillations and pattern formation in

*Corresponding author. Email: lebiedz@iwr.uni-heidelberg.de

Mathematical and Computer Modelling of Dynamical Systems
ISSN 1387-3954 print/ISSN 1744-5051 online © 2007 Taylor & Francis
http://www.tandf.co.uk/journals
DOI: 10.1080/13873950701243969

space and time are believed to be important players in the huge variety of dynamical mechanisms of cellular processes. Advanced mathematical methods are essential, not only for numerical simulation but also for model analysis.

Optimal control, for example, is a promising tool to analyse how dynamic perturbations of a given system might look like to achieve an observed or desired dynamical behaviour. In this article, we will concentrate on two different aspects of how optimal control can be exploited in biological and biochemical modelling. The first aspect is the formulation and solution of inverse problems to detect appropriate temporally varying input signals leading to specific experimentally measured output. The second is the control of self-organized processes by target-oriented external manipulation to induce desired behaviour. In the future, the latter approach might be valuable for the development of drugs and treatment strategies aimed at so-called dynamic diseases that are caused by malfunctions in the dynamics of cellular signalling and metabolism. Due to the challenges posed by numerical optimal control of self-organized systems displaying pattern formation in time (and space) involving inherent unstable dynamical modes, the use, adaptation and extension of elaborate and efficient optimization techniques are important issues. In this article, we apply state-of-the-art optimal control methods based on multiple shooting for the solution of inverse problems with time-dependent input controls for ODE/DAE and present the application of a novel multiple-shooting mixed-integer approach to a bang-bang control scenario aimed at annihilation of biochemical oscillators.

2. Glycolysis oscillations in immune cells

2.1 *Neutrophils in immune defence*

In this section, we will demonstrate how optimal control methods can be used to gain insight into possible cellular signalling routes. Cells react and adapt to changes in their environment by relaying information through signal transduction pathways. The spatiotemporal dynamics of the signalling routes encode transduced information and modelling and simulation techniques integrating quantitative *in vivo* experimental data are believed to be crucial on the way towards an elucidation of the enormous complexity of signalling mechanisms. Neutrophils are cells of the human immune system and exhibit central functions in the first line of defence against inflammation. Their major role is the detection, internalization (phagocytosis), and digestion of invading pathogens. While normally circulating in the blood stream, at sites of inflammation they adhere to endothelial cells that form the blood vessel wall and polarize, acquiring a flat, elongated shape. Then they leave the vascular system (extravasation) and migrate actively, stimulated by chemotactic factors, towards the centre of tissue inflammation where they engulf the target pathogens. The destruction of pathogens is supported by synthesis and release of reactive oxygen species leading to degradation of the foreign biomaterial. Because of their autonomous functions without being integrated in tissue, neutrophils are ideal objects for single cell studies of signalling mechanisms and the associated physiology. A thorough understanding of the signal transduction involved in polarization, direction finding, and pathogen targeting of neutrophils by help of spatiotemporal mathematical modelling and simulation may have the long-term potential to lead to medical applications in immunology.

Recently, signalling processes involving biochemical oscillations and highly asymmetric and localized Ca^{2+} waves [2] and metabolic NAD(P)H (Nicotinamid-adenine-dinucleotide and its phosphate) waves [3] have been observed which correlate with orientation and migration of neutrophils following chemotactic stimulation as well as specific targeting of pathogens by reactive oxygen intermediates (ROI). In these studies, high-speed fluorescence microscopy has been used to track Ca^{2+} in polarized, adherent neutrophils. Every 20 s, a concentration spike occurs, a Ca^{2+} wave departs from the front (lamellipodium) of a polarized neutrophil, travels along the inner perimeter of the cell membrane in counterclockwise direction until the point of departure is reached. When the chemotactic factor fMLP is applied locally to the cell membrane, the frequency of Ca^{2+} spikes increases to 10 s and the counterclockwise wave splits at the fMLP binding site, emitting a second wave travelling in a similar fashion in clockwise direction. These two waves cross at the other end of the cell and continue propagation until they again reach the fMLP binding site where they both terminate. Eventually, by rearrangement of the cellular shape, this site becomes the new lamellipodium and determines the new direction of active movement. Thus, the observed signalling routes seem to be involved in early events related to cellular orientation and direction finding.

In addition to the calcium waves, metabolic NAD(P)H oscillations and waves are observed in adherent, polarized neutrophils. These propagate unidirectionally from the rear to the front of the cell. A well-defined phase relation between corresponding NAD(P)H oscillations and calcium spikes suggests a direct correlation between the signalling apparatus and cell metabolism. The NAD(P)H waves obviously drive the target-oriented "'shooting" of reactive oxygen towards pathogens by spatiotemporally controlling the activity of the enzyme NAD(P)H oxidase located in the cell membrane. After chemoattractant stimulation, the NAD(P)H oscillation frequency reduplicates and the wave splits in the middle of the cell into two counter-propagating waves that are now reflected at front and rear end plasma membrane and cross each other unaffectedly. The mechanism and the function of oscillations and waves and the increase of the frequency upon activation are unknown.

Given the fact that the metabolism of neutrophils relies heavily on anaerobic degradation of glucose, the assumption that glycolysis is at the core of the oscillations is reasonable since glycolysis produces NADH and is known to be able to display oscillatory kinetics [4]. It is known that transport of glucose into the cell is variable and after activation of the neutrophils an increase of glucose-transport into the cell is observed experimentally [5]. Our hypothesis is therefore that a dynamically regulated influx of glucose may control self-organized dynamics in neutrophil metabolism.

2.2 *Modelling and optimal control*

Glycolysis is composed of a series of reactions which step-wise convert glucose to pyruvate. It is the central part of the general cellular energy metabolism and consists of 11 reactions which are catalyzed by enzymes.

A scheme of the major part of the reaction pathway is depicted in figure 1. The model equations are based on a model for neutrophilic glycolysis [7]. The model is based on [8] and [9] and directly relates to experimental *in vivo* data. The full model-equations are given in Appendix A. Exemplarily, we provide the rate equation for the

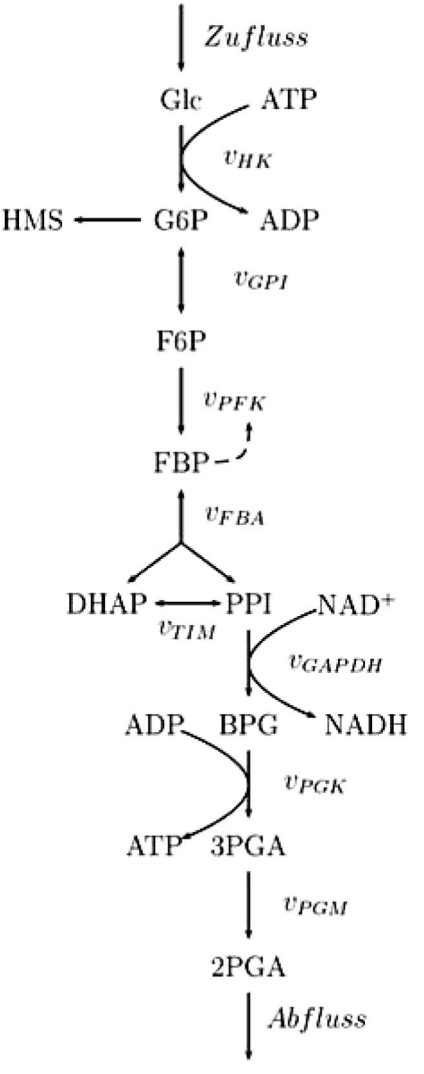

Figure 1. Scheme of the major part of glycolysis captured by our kinetic ODE model. *v* describes the reaction rates of the indexed enzymes. A part of the G6P flows into a branching pathway, the hexosemonophosphateshunt, which is not modelled explicitly but by assuming a first-order leakage of G6P. For explanation of the chemical species see for example [6].

most important reaction which is catalyzed by the enzyme phosphofructokinase (PFK). For the PFK reaction an allosteric regulation of the enzyme by its product FBP is known which leads to sigmoidal saturation kinetics. This can be modelled by an extended Hill-equation [10] of the form

$$v_{\mathrm{PFK}} = \frac{V_{\mathrm{pfk}} \left(\frac{[\mathrm{F6P}]}{K_{\mathrm{pfk}}}\right)^{\mathrm{h_{pfk}}}}{\left(\frac{[\mathrm{F6P}]}{K_{\mathrm{pfk}}}\right)^{\mathrm{h_{pfk}}} + \frac{1+\left(\frac{k_{\mathrm{X}}[\mathrm{FBP}]}{K_{\mathrm{fba}}}\right)^{\mathrm{h_{fba}}}}{1+\alpha^{\mathrm{h}}\left(\frac{k_{\mathrm{X}}[\mathrm{FBP}]}{K_{\mathrm{fba}}}\right)^{\mathrm{h_{fba}}}}}, \tag{1}$$

with a variable Hill coefficient

$$h^*_{\mathrm{pfk}} = h_{\mathrm{pfk}} - \underbrace{(h_{\mathrm{pfk}} - h_{\mathrm{act}})}_{\sigma}\left(\frac{\frac{[\mathrm{FBP}]}{K_{\mathrm{fba}}}}{1+\frac{[\mathrm{FBP}]}{K_{\mathrm{fba}}}}\right). \tag{2}$$

For a detailed explanation of kinetic constants and the modelling itself which is beyond the scope of this work we have to refer to [7]. With the full model the oscillations of an adherent neutrophil with a period in the range of 20 s can be simulated (see figure 2(a)).

However, the simulated periodic NADH concentrations do not have the experimentally observed harmonic sine shape [12] but are rather oscillations of the relaxation type. They cannot be fitted to experimental results in a biochemically reasonable range of parameter values.

Here, our aim is to demonstrate that the oscillations might be dynamically controlled by variable glucose influx $u(t)$ giving rise to the observed shape. For that purpose, we consider the following optimal control problem with periodic boundary conditions and fixed end time appropriately chosen near the experimentally observed value for three oscillation periods:

$$\min_{\mathrm{c,u}} \int_0^{T=60} (c_{\mathrm{NADH}}(t) - \bar{c}(t))^2 dt$$

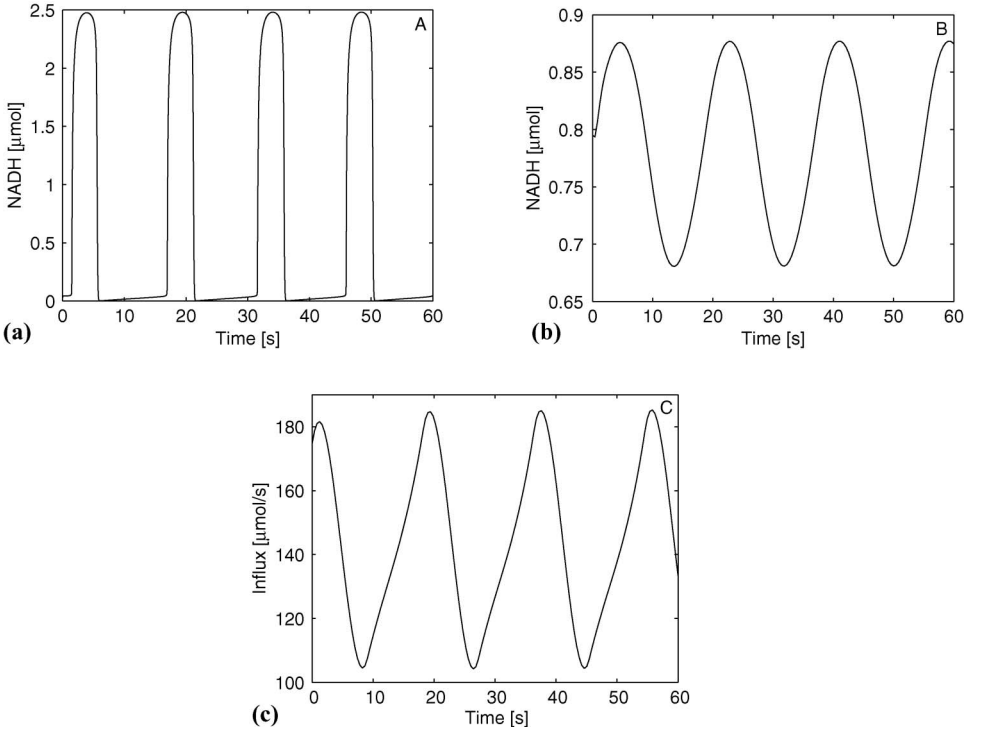

Figure 2. (a) Simulation of the glycolysis model with relaxation-type shape of the oscillations (numerical integration with the BDF-code DAESOL [11]). (b) Induced NADH oscillations with dynamical glucose influx computed as a solution of the optimal control problem. (c) Optimal control function: glucose influx $u(t)$.

subject to

$$\dot{c}(t) = f_{\text{Glyco}}(t, c(t), u(t)), \quad c(t) \in [0, c_{\max}], t \in [0, 60]$$
$$c(t) \geq 0. \tag{3}$$

The vector $c(t) \in \mathbb{R}^9$ denotes the considered metabolite concentrations and $u \in \mathbb{R}^1$ represents a dynamical influx of glucose. $\bar{c}(t)$ is a sine function $a \sin(bt + d) + e$ with the parameters $a = 0.1$, $b = 0.345$, $d = 0$, and $e = 0.785$ to which the NADH oscillations are supposed to be fitted. These values are experimentally motivated [12] and account for the range of relative oscillation amplitude and frequency. The additional inequality constraints for the metabolite concentrations are obviously physically motivated.

The optimal solution of this problem is computed by the direct multiple shooting (DMS) code MUSCOD-II [13] with a piecewise polynomial discretization of the control functions. More methodical details on DMS can be found in Section 4. The obtained optimal control and the corresponding oscillating optimal trajectory are shown in figures 2(b) and 2(c).

Interestingly, the obtained control and the induced oscillations have a phase difference of approximately 90°. This is the same phase shift observed between NAD(P)H and Ca^{2+} oscillations in experiments [12]. Because of the detected phase relation between optimal control input (dynamic glucose influx) and system response (desired shape of NADH oscillations) and the correlation with Ca^{2+}-oscillations, we argue that the NAD(P)H oscillations may be controlled by calcium signals. Calcium is well known as a messenger in signal transduction and information can be encoded in its dynamic characteristics like frequency and amplitude of oscillations [14]. In our case, a hypothetical mechanism underlying the correlation between calcium and NAD(P)H oscillations could be that glucose transporters in the plasma membrane of the cell are activated by increased calcium concentration. This is supported by some experimental data, see e.g. [15] for an early study.

3. Optimal control of the circadian clock

3.1 *Rhythms in biology*

In the second part of the article, we present optimal control results for another biological rhythm, the circadian clock, and apply a novel approach related to mixed-integer optimal control to obtain bang-bang solutions. Rhythmic processes are encountered at all levels of biological organization and are a subject of great interest for both biological and mathematical research communities (see e.g. the review [16]). The role of circadian rhythms with a period of nearly 24 h is of particular importance because many physiological and behavioural functions of living creatures, ranging from insects to mammals, appear to be governed by this so-called "master clock". The pacemaker delivers a circadian rhythm, generated by periodic activation/inhibition of transcription of a set of genes, denoted as "clock genes". The molecular basis of these mechanisms has been clarified over the past decade, first for an insect, the fruit fly Drosophila, and more recently also for mammals (see [17] for a review). The central mechanism seems to be conserved and is based on a feedback regulated gene transcription network in the cell nucleus and its corresponding protein translation products in the cytoplasm. Some of the most intriguing observations related to circadian rhythms are that they seem to be entrained by periodic light and darkness

periods, persist under conditions of complete darkness and can be modified (phase shifted) by external light pulses. In particular, well-defined suppression and restoration of circadian rhythms are interesting scenarios to be studied. However, neither the phase at which stimuli for suppression or restoration of oscillations have to be applied nor the characteristics of the critical stimulus strength are *a priori* clear. Winfree proposed an approach to determine these parameters by probing the phase resetting response for various stimulus intensities and corresponding phase relations between stimulus and system state and construction of so-called phase resetting curves [18]. Here, we demonstrate how model-based optimal control of mixed-integer type can be exploited for the task of systematically finding appropriate strength and timing of critical external stimuli leading to specific suppression and restoration of circadian rhythms. To our knowledge, this is the first application of mixed-integer optimal control to systematic phase shift of circadian rhythms by light.

3.2 *Model*

One of the most reliable detailed models available for the circadian clock is based on experimental observations collected for Drosophila, a widely used model organism in biology; the model [19] (schematized in figure 3) is centred around negative auto-regulation of gene expression.

It takes into account nuclear transcription of the *per* and *tim* genes and transport of the *per* and *tim* mRNAs into the cytoplasm, where they are translated into PER and TIM proteins. The latter can be multiply phosphorylated and form a complex that enters the nucleus and represses *per* and *tim* transcription. The model incorporates degradation of the PER and TIM proteins and their mRNAs. Light influences the Drosophila clock by triggering TIM degradation [20], the maximum rate of TIM degradation v_{dT} increases with increasing light intensity. (In mammals, where *per* and *tim* genes are also found, light acts by enhancing the rate of *per* expression v_{sP}.) The Drosophila model is described by a set of 10 ordinary differential equations (ODE) that govern the time evolution of the concentrations of *per* and *tim* mRNAs and of the various forms of PER and TIM proteins and the PER–TIM complex [19]. The model can reproduce circadian oscillations in continuous darkness, entrainment by light–dark cycles, and phase shifting by light pulses. The full model-equations are given in Appendix B.

On the basis of this model, we consider suppression of circadian rhythmicity by directly controlling the light-sensitive parameter v_{dT}. The aim of our control approach is to identify strength and timing of the light-induced parameter changes for TIM protein degradation corresponding to a phase singularity which suppresses the circadian rhythms immediately. We address this problem by model-based mixed-integer optimal control via formulation of the control objective as the minimization of the system state deviation from the desired steady state integrated over time. We are interested, in particular, in control functions v_{dT} that switch once between the value $v_{\mathrm{dT}} = v_{\mathrm{dT}_{\mathrm{min}}}$ and $v_{\mathrm{dT}} = v_{\mathrm{dT}_{\mathrm{max}}}$, corresponding to a maximum amount of light and once back to the background intensity (bang-bang control). By setting $v_{\mathrm{dT}}(t) = v_{\mathrm{dT}_{\mathrm{min}}} + w(t)(v_{\mathrm{dT}_{\mathrm{max}}} - v_{\mathrm{dT}_{\mathrm{min}}})$ this can be formulated assuming a binary-valued control function $w(t)$ which can take only boundary values low or up of a relaxed feasible domain [0,1]. The corresponding mixed-integer optimal control problem is

$$\min_{w(t)} J(x, w(t)) := \int_0^T \sum_{\mathrm{i}=1}^{10} (x_i(t, w(t)) - x_{\mathrm{i}}^s)^2 dt \tag{4}$$

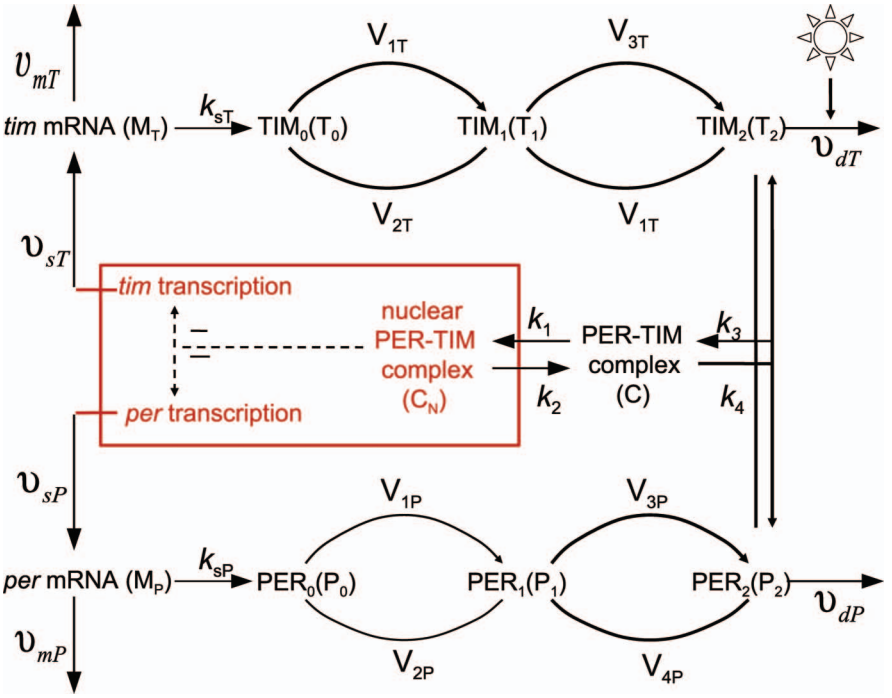

Figure 3. Model for circadian oscillator in Drosophila involving negative regulation of gene expression by PER and TIM. *per* (M_P) and *tim* (M_T) mRNAs are synthesized in the nucleus and transferred into the cytoplasm, where they accumulate at the maximum rates v_{sP} and v_{sT}, respectively. There they are degraded enzymatically at the maximum rates, v_{mP} and v_{mT}, with the Michaelis-Menten constants, K_{mP} and K_{mT}. The rates of synthesis of the PER and TIM proteins are proportional to M_P and M_T characterized by the apparent first-order rate constants k_{sP} and k_{sT}. Parameters $V_{iP}(V_{iT})$ and $K_{iP}(K_{iT})$ (i = 1,...,4) denote the maximum rate and Michaelis constant of the kinases and phosphatases involved in the reversible phosphorylation of P_0 (T_0) into P_1 (T_1) and P_1 (T_1) into P_2 (T_2), respectively. The fully phosphorylated forms (P_2 and T_2) are degraded by enzymes with maximum rate $\{v_{dP}$ and v_{dT} and Michaelis-Menten constants K_{dP} and K_{dT} and reversibly form a complex C (association and dissociation are characterized by the rate constants k_3 and k_4), which is transported into the nucleus at a rate characterized by the apparent first-order rate constant k_1. Transport of the nuclear form of the PER-TIM complex (C_N) into the cytoplasm is described by the apparent first-order rate constant k_2. The negative feedback exerted by the nuclear PER-TIM complex on *per* and *tim* transcription is modelled by a Hill-type equation. For the full kinetic model equations see [19].

subject to the ODEs, the integer constraints $w(t) \in \{0,1\}$, positive valued concentrations $x_i(t)$, and initial conditions. The vector x_i^sdenotes the steady state coordinates. For rhythm restoration, a maximization of the same objective functional turned out to be suitable.

In the uncontrolled case, the model shows endogenous limit-cycle oscillations with a period of approximately 24 h in a numerical simulation for the chosen parameter values [19]. A bifurcation analysis of the model (not shown) reveals a bistability region in the range of the applied basal background illumination strength, namely, the coexistence of a stable steady state and a stable limit cycle after a Hopf-bifurcation. This situation is important to obtain stability in our open-loop control scenarios aimed at switching between the periodic and stationary states.

For limit-cycle attractors surrounding a steady state, Winfree has proven via topological arguments under very general assumptions that a critical stimulus with appropriate timing, length, and strength corresponding to a so-called phase singularity must exist which takes the system immediately to steady state, meaning instantaneous suppression of the oscillations [18]. We apply a novel approach based on the direct

multiple shooting method (DMS) [21] which can treat bang-bang control scenarios with a piecewise constant control parameterization to obtain such an optimal light stimulus to suppress and subsequently restore the circadian rhythm in the Drosophila model at *a priori* defined time points. We compute an optimal control $v_{dT}(t)$ as a solution of problem (4) via convex relaxation of the integer constraints. The result is shown in figure 4(a). Obviously the rhythm can be suppressed and restored by adjustable time-varying light pulses. However, these are difficult to realize in practice. Therefore, we go on to compute a bang-bang solution of problem (4) (see figure 4(b)). Figure 5 shows the corresponding controlled system state trajectory for the TIM protein concentration. Obviously, it is possible to achieve a well-defined optimal switching between stationary and oscillatory states on the basis of the circadian rhythm model.

4. Numerical methods for optimal control

There are various methods in the literature to solve optimal control problems for ODE/DAE. We choose Bock's direct multiple shooting method, [21], as this approach has proven to be a reliable tool not only for mechanics and chemical engineering, but also in systems biology of self-organization, e.g. [22], [23]. It is a direct method and therefore based on a transformation of the infinite–dimensional control problem

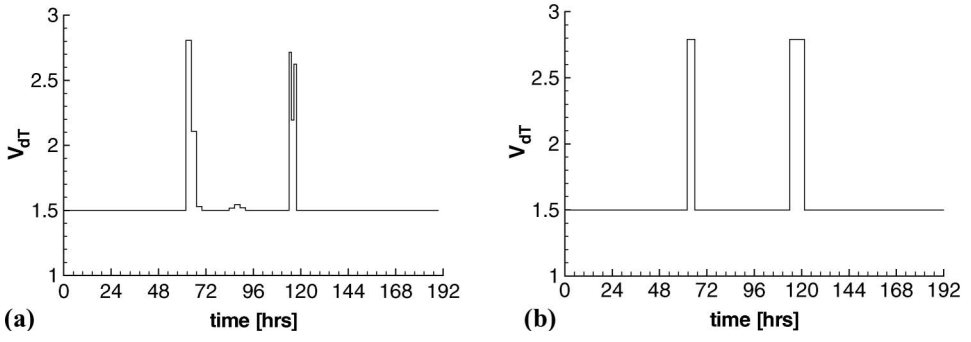

Figure 4. Optimal control for the relaxed problem (a) and the bang-bang problem (b) of circadian rhythm suppression by light and subsequent restoration of the rhythm based on the Drosophila model. Control input: light-sensitive maximum rate of protein degradation v_{dT} as a function of time.

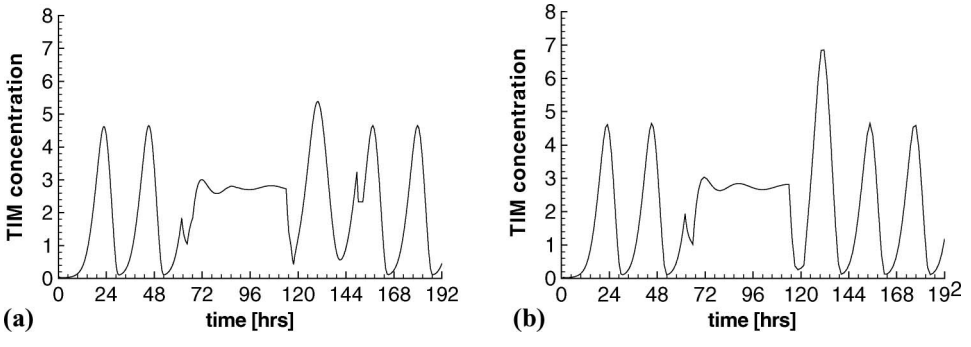

Figure 5. Rhythm suppression by a light stimuli corresponding to the optimal control functions in figure 4, (a) relaxed control scenario, (b) bang-bang control scenario. The plot shows the TIM protein concentration in nM as a function of time.

to a finite–dimensional nonlinear program (NLP) by a discretization of the control functions. A time grid of *multiple shooting nodes* is introduced,

$$0 \leq t_1 \leq \cdots \leq t_{n_{\mathrm{ms}}} = T. \tag{5}$$

With finitely many control parameters $q_i \in \mathbb{R}^{n_i}$,

$$q = (q_0, q_1, \ldots, q_{n_{\mathrm{ms}}-1})^T,$$

a piecewise approximation $\hat{u}$ of the control functions u on the grid (5) is then defined by

$$\hat{u}(t) = \varphi_i(t, q_i), \quad t \in [t_i, t_{i+1}], \quad i = 0, \ldots, n_{\mathrm{ms}} - 1. \tag{6}$$

In practice, the functions φ_i are typically vectors of constant or linear functions. On the grid (5) node values $s_i^x \approx x(t_i) \in \mathbb{R}^{n_x}$ are introduced, from now on $0 \leq i < n_{\mathrm{ms}}$, that serve as initial values of intermediate trajectories. All values $x(t)$ in between the grid points are obtained by a decoupled integration with an ODE/DAE solver on each of the multiple shooting intervals. Continuity of the state trajectory at the multiple shooting grid points

$$s_{i+1}^x = x(t_{i+1}; s_i^x, q_i, p) \tag{7}$$

is incorporated via equality constraints into the NLP. Here $x(\cdot)$ denotes the solution of the ODE on interval $[t_i,\ t_i + 1]$ with initial values s_i^x at time t_i. Figure 6 illustrates the concept of direct multiple shooting. The control variables q_i, the global parameters p, that may include the time horizon length $h = t_f - t_0$ for problems with free end time, and the node values s_i^x are the degrees of freedom of the discretized and parameterized optimal control problem. If we write them in one n_ξ-dimensional vector

$$\xi = (s_0^x, q_0, s_1^x, \ldots, q_{n_{\mathrm{ms}}-1}, s_{n_{\mathrm{ms}}}^x, p)^T, \tag{8}$$

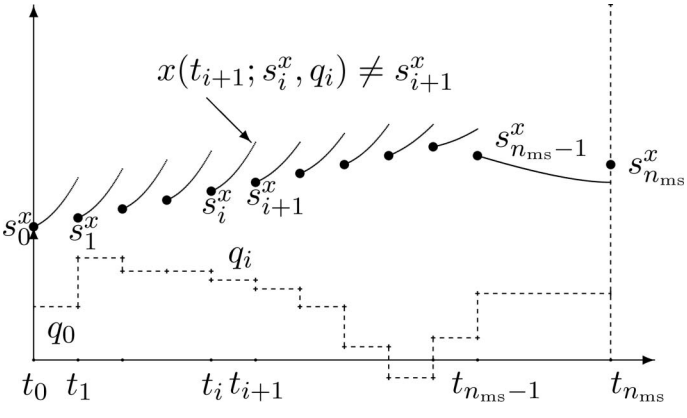

Figure 6. Illustration of direct multiple shooting during SQP iterations. The controls are discretized, the corresponding states obtained by piecewise integration. The matching conditions are violated in this scheme—the overall trajectory is not yet continuous.

subsuming all equality constraints and continuity conditions (7) in a function $G(\xi)$ and all inequality constraints in a function $H(\xi)$, the resulting NLP can be formulated as

$$\min_{\xi} \quad F(\xi) \tag{9}$$

$$\text{s.t.} \quad G(\xi) = 0, \tag{10}$$

$$H(\xi) \leq 0. \tag{11}$$

This NLP can be solved with tailored iterative methods exploiting the structure of the problem, e.g. by sequential quadratic programming (SQP). The continuity conditions do not necessarily have to be satisfied during the iterations of the SQP algorithm used to solve the NLP, but surely when convergence has been achieved. Direct multiple shooting is therefore a so-called all–at–once approach that solves the dynamic equations and the optimization problem at the same time opposed to the sequential approach of single shooting that computes a continuous trajectory as a feasible ODE/DAE solution in every iteration. For more details on direct multiple shooting, see [21] or [13]. If the optimal control problem under consideration contains control functions $w(\cdot)$ with a restriction to values in a disjoint set, say to $\{0, 1\}^{n_w}$, the methods have to be extended. We say that a trajectory $\mathcal{T} = (x, w, u, p)$ is binary feasible, if all constraints are fulfilled and $w(t) \in \{0, 1\}^{n_w}$ for all $t \in [t_0, t_f]$. For the application treated in this article, we apply the novel algorithm MSMINTOC introduced in [24] that can be sketched as follows. We relax the control functions to $w(\cdot) \in [0,1]^{n_w}$. We solve the relaxed problem for a given control discretization $\mathcal{G}^0$ and obtain the grid–dependent optimal function value $\Phi^{\mathrm{RL}}_{\mathcal{G}^0}$. We iterate on a refinement of the grid for n_{ext} steps with the idea to extrapolate towards $n_{\mathrm{ms}} \mapsto \infty$. We obtain $\Phi^{\mathrm{RL}} = \Phi^{\mathrm{RL}}_{\mathcal{G}^{n_{\mathrm{ext}}}}$ as the objective function value on the finest grid $\mathcal{G}^{n_{\mathrm{ext}}}$. This objective function value serves as a lower bound that can be approximated up to any user–specified tolerance $\varepsilon > 0$ by a binary admissible trajectory, for a proof see [24]. If the optimal trajectory on $\mathcal{G}^{n_{\mathrm{ext}}}$ is already binary admissible then stop. Otherwise apply a rounding or penalty heuristics on the grid. If the trajectory is binary admissible, obtain an upper bound Φ^{ROU}. If $\Phi^{ROU} < \Phi^{RL} + \varepsilon$ then stop. Otherwise optimize the switching times for a fixed switching structure, initialized with the trajectory obtained by heuristics. Again, if the obtained trajectory is binary admissible, obtain an upper bound Φ^{STO} and if $\Phi^{STO} < \Phi^{RL} + \varepsilon$ then stop. For most practical problems and the model under consideration in this study a modest iteration on n_{ext} is sufficient to obtain a binary admissible trajectory that is within a certain tolerance to the reachable objective function value. If this is not the case, a further interplay between a tailored rounding strategy with an adaptive refinement of the control discretization grid or even a rigorous determination of the global solution on a grid by, e.g. Branch & Bound is necessary. See [24] for details, proofs and applications.

5. Conclusion

In this article, we demonstrate how optimal control can be used in biochemical modelling. We discuss optimal control first as a means to analyse potential dynamic signalling functions and second to compute external perturbations in order to obtain a specific desired behaviour. In particular, the understanding of the role of specific self-organization and its control will be of fundamental interest because various

experimental observations suggest that information is encoded in different shape of the temporal and spatiotemporal patterns which may be eventually exploited even for drug development [25]. In this context, the example application to circadian rhythms is interesting *per se* because circadian rhythms seem to be related to the regular cycles of cell division which are both malfunctioning in many tumour cells [26] giving rise to uncontrollably proliferating cancer.

Acknowledgements

The authors thank Jürgen Warnatz and Hans-Georg Bock (IWR, Heidelberg) for support and funding.

References

[1] Glansdorff, P. and Prigogine, I., 1971, *Thermodynamic Theory of Structure, Stability and Fluctuations*, (New York: Wiley).
[2] Kindzelskii, A.L. and Petty, H.R., 2003, Intracellular calcium waves accompany neutrophil polarization, formylmethionylleucylphenylalanine stimulation, and phagocytosis: a high speed microscopy study. *Journal of Immunology*, **170**, 64–72.
[3] Petty, H.R. and Kindzelskii, A.L., 2002, Dissipative metabolic patterns respond during neutrophil transmembrane signaling. *Proceedings of the National Academy of Sciences USA*, **98**, 3145–3149.
[4] Goldbeter, A., 1996, *Biochemical Oscillations and Cellular Rhythms: The molecular bases of periodic and chaotic behaviour* (Cambridge: Cambridge University Press).
[5] Tan, A.S., Ahmed, N. and Berridge, M., 1998, Acute regulation of glucose transport after activation of human peripheral blood neutrophils by phorbol myristate acetate, fMLP, and granulocyte-macrophage colony-stimulating factor. *Blood*, **91**, 649–655.
[6] Campell, N.A. and Reece, J.B., 2005, *Biology* (San Francisco: Pearson Education).
[7] Kummer, U., Zobeley, J., Brasen, J.C., Fahmy, R., Kindzelskii, A.L., Petty, A.R., Clark, A.J. and Petty, H.R., 2007, Elevated glucose concentrations promote receptor-independent activation of adherent human neutrophils: an experimental and computational approach. *Biophysical Journal*, **92**, 2597–2607.
[8] Westermark, P.O. and Lansner, A., 2003, A model of phosphofructokinase and glycolytic oscillations in the pancreatic β-cells. *Biophysical Journal*, **85**, 126–139.
[9] Mulquiney, P.J. and Kuchel, P.W., 1999, Model of 2,3-bisphosphoglycerate metabolism in the human erythrocyte based on detailed enzyme kinetic equations: equations and parameter refinement. *Biochemical Journal*, **342**, 581–596.
[10] Bisswanger, H., 2002, *Enzyme Kinetics* (Weinheim: Wiley-VCH).
[11] Bauer, I., Finocchi, F., Duschl, W.J., Gail, H.P. and Schlöder, J.P., 1997, Simulation of chemical reactions and dust destruction in protoplanetary accretion discs. *Astronomy and Astrophysics*, **317**, 273–289.
[12] Petty, H.R., 2000, Oscillatory signals in migrating neutrophils: effects of time-varying chemical and electric fields. In: J. Walleczek (Ed.), *Self-Organized Biological Dynamics & Nonlinear Control* (Cambridge: Cambridge University Press).
[13] Leineweber, D.B., Bauer, I., Bock, H.G. and Schlöder, J.P., 2003, An efficient multiple shooting based reduced SQP strategy for large-scale dynamic process optimization. Part I: Theoretical aspects. *Computers and Chemical Engineering*, **27**, 157–166.
[14] Berridge, M., 1997, The AM and FM of calcium signalling. *Nature*, **386**, 759–760.
[15] O'Flaherty, J.T., Cousart, S., Swendsen, C.L., DeChatelet, L.R., Bass, D.A., Love, S.H. and McCall, C.E., 1981, Role of Ca2+ and Mg2+ in neutrophil hexose transport. *Biochimica et Biophysica Acta*, **640**, 223–230.
[16] Goldbeter, A., 2002, Computational approaches to cellular rhythms. *Nature*, **420**, 238–245.
[17] Reppert, S.M. and Weaver, D.R., 2002, Coordination of circadian timing in mammals. *Nature*, **418**, 935–941.
[18] Winfree, A.T., 2001, *The Geometry of Biological Time* (New York: Springer).
[19] Leloup, J.C. and Goldbeter, A., 1998, A model for circadian rhythms in Drosophila incorporating the formation of a complex between the PER and TIM proteins. *Journal of Biological Rhythms*, **13**, 70–87.
[20] Hunter-Ensor, M., Ousley, A. and Sehgal, A., 1996, Regulation of the Drosophila protein timeless suggests a mechanism for resetting the circadian clock by light. *Cell*, **84**, 677–685.
[21] Bock, H.G. and Plitt, K.J., 1984, A multiple shooting algorithm for direct solution of optimal control problems. In: *Proceedings of the 9th IFAC World Congress* (Budapest: Pergamon), pp. 243–247.

[22] Lebiedz, D. and Brandt-Pollmann, U., 2003, Manipulation of self-aggregation patterns and waves in a reaction-diffusion system by optimal boundary control strategies. *Physical Review Letters*, **91**, 208301.
[23] Lebiedz, D., Sager, S., Bock, H.G. and Lebiedz, P., 2005, Annihilation of limit cycle oscillations by identification of critical perturbing stimuli via mixed-integer optimal control. *Physical Review Letters*, **95**, 108303.
[24] Sager, S., 2005, *Numerical methods for mixed–integer optimal control problems* (Tönning, Lübeck, Marburg: Der andere Verlag).
[25] Petty, H.R., 2004, Dynamic chemical instabilities in living cells may provide a novel route in drug development. *Chembiochem*, **5**, 1359–1364.
[26] Fu, L. and Lee, C.C., 2003, The circadian clock: pacemaker and tumor suppressor. *Nature Reviews Cancer*, **3**, 350–361.

Appendix A: Glycolysis model-equations and rate-constants

$$\frac{d[\mathrm{Glc}]}{dt} = \mathrm{Zufluss} - \mathrm{HK}$$
$$\frac{d[\mathrm{G6P}]}{dt} = \mathrm{HK} - \mathrm{GPI} - k_{\mathrm{HMS}}[\mathrm{G6P}]$$
$$\frac{d[\mathrm{F6P}]}{dt} = \mathrm{GPI} - \mathrm{PFK}$$
$$\frac{d[\mathrm{FBP}]}{dt} = \mathrm{PFK} - \mathrm{FBA}$$
$$\frac{d[\mathrm{PPI}]}{dt} = 2\ \mathrm{FBA} - \mathrm{GAPDH}$$
$$\frac{d[\mathrm{BPG}]}{dt} = \mathrm{GAPDH} - \mathrm{PGK}$$
$$\frac{d[\mathrm{3PGA}]}{dt} = \mathrm{PGK} - \mathrm{PGM}$$
$$\frac{d[\mathrm{2PGA}]}{dt} = \mathrm{PGM} - k_{\mathrm{ab}}[\mathrm{2PGA}]$$
$$\frac{d[\mathrm{NADH}]}{dt} = \mathrm{GAPDH} - k_{\mathrm{NADH}}[\mathrm{NADH}]$$

with the reaction equations

$$\mathrm{HK} = \frac{V_{\mathrm{hk}}[\mathrm{Glc}]}{K_{\mathrm{hk}} + [\mathrm{Glc}]}$$
$$\mathrm{GPI} = k_{\mathrm{gpi}}[\mathrm{G6P}] - k_{\mathrm{gpir}}[\mathrm{F6P}]$$
$$\mathrm{PFK} = \frac{V_{\mathrm{pfk}}\left(\frac{[\mathrm{F6P}]}{K_{\mathrm{pfk}}}\right)^{h_{\mathrm{pfk}} - \sigma\left(\frac{\frac{[\mathrm{FBP}]}{K_{\mathrm{fba}}}}{1+\frac{[\mathrm{FBP}]}{K_{\mathrm{fba}}}}\right)}}{\left(\frac{[\mathrm{F6P}]}{K_{\mathrm{pfk}}}\right)^{h_{\mathrm{pfk}} - \sigma\left(\frac{\frac{[\mathrm{FBP}]}{K_{\mathrm{fba}}}}{1+\frac{[\mathrm{FBP}]}{K_{\mathrm{fba}}}}\right)} + \frac{1+\left(\frac{k_{\mathrm{x}}[\mathrm{FBP}]}{K_{\mathrm{fba}}}\right)^{h_{\mathrm{fba}}}}{1+\alpha^{\mathrm{h}}\left(\frac{k_{\mathrm{x}}[\mathrm{FBP}]}{K_{\mathrm{fba}}}\right)^{h_{\mathrm{fba}}}}}$$
$$\mathrm{FBA} = \frac{V_{\mathrm{fba}}[\mathrm{FBP}]}{K_{\mathrm{fba}} + [\mathrm{FBP}]}$$
$$\mathrm{GAPDH} = \frac{V_{\mathrm{gapdh}}[\mathrm{PPI}][\mathrm{NAD}^+]}{K_1K_2K_3[\mathrm{PPI}]\left(1 + \frac{[\mathrm{PPI}]}{K_3'}\right) + K_3\overline{[\mathrm{P_i}]}[\mathrm{NAD}^+]}$$

$$+\frac{K_1K_2[\mathrm{NAD^+}][\mathrm{PPI}]}{K_{i_2}}+K_2[\mathrm{PPI}](1+\frac{[\mathrm{PPI}]}{K'_3})+\overline{[\mathrm{P_i}]}[\mathrm{NAD^+}][\mathrm{PPI}]}$$

$$\mathrm{PGK}=\frac{V_{\mathrm{pgk}}[\mathrm{BPG}]}{K_{\mathrm{iADP}}K_{\mathrm{pgk}}+\frac{K_{\mathrm{pgk}}K_{\mathrm{iADP}}[\mathrm{BPG}]}{K_{\mathrm{iBPG}}}+\overline{[\mathrm{ADP}]}K_{\mathrm{pgk}}+\overline{[\mathrm{ADP}]}[\mathrm{BPG}]}$$

$$\mathrm{PGM}=\frac{V_{\mathrm{fpgm}}[3\mathrm{PGA}]-V_{\mathrm{rpgm}}[2\mathrm{PGA}]}{K_{3\mathrm{PGA}}K_{2\mathrm{PGA}}+[3\mathrm{PGA}]K_{2\mathrm{PGA}}+[2\mathrm{PGA}]K_{3\mathrm{PGA}}}$$

Table A1. Rate constants for the Glycolysis model.

Kinetic parameter	Parameter value
V_{HK}	170 μmol
k_{gpi}	1800 s^{-1}
V_{pfk}	2220 μmol
k_{x}	10
K_{fba}	5 μmol
h_{pfk}	2.5
V_{fba}	200 μmol
K_1	3160 μmol
K_3	95 μmol
K_{i_2}	45 μmol
K_{iadp}	80 μmol
K_{ibpg}	1600 μmol
V_{fpgm}	6600 μmol
$K_{3\mathrm{pga}}$	168 μmol
k_{NADH}	155 s^{-1}
k_{HMS}	0.5 s^{-1}
c_{sum}	60 μmol
K_{HK}	47 μmol
k_{gpir}	2100 s^{-1}
K_{pfk}	4000 μmol
h_{fba}	2.5
α	5
σ	1.5
V_{gapdh}	1.103 10^7 μmol
K_2	45 μmol
K'_{ppi}	31 μmol
V_{pgk}	120 000 μmol
K_{bpg}	2 μmol
$\overline{[\mathrm{ADP}]}$	110 μmol
V_{rpgm}	5900 μmol
$K_{2\mathrm{pga}}$	14 μmol
k_{ab}	0.1 s^{-1}
$\overline{[P_i]}$	1000 μmol

Appendix B: Drosophila model-equations and rate-constants

$$\frac{dM_{\mathrm{p}}}{dt}=v_{\mathrm{sP}}\frac{K_{\mathrm{IP}}{}^n}{K_{\mathrm{IP}}{}^n+C_{\mathrm{N}}{}^n}-v_{\mathrm{mP}}\frac{M_{\mathrm{P}}}{K_{\mathrm{mP}}+M_{\mathrm{P}}}-k_{\mathrm{d}}M_{\mathrm{P}}$$

$$\frac{dP_0}{dt}=k_{\mathrm{sP}}M_{\mathrm{P}}-V_{1\mathrm{P}}\frac{P_0}{K_{1\mathrm{P}}+P_0}+V_{2\mathrm{P}}\frac{P_1}{K_{2\mathrm{P}}+P_1}-k_{\mathrm{d}}P_0$$

$$\frac{dP_1}{dt}=V_{1\mathrm{P}}\frac{P_0}{K_{1\mathrm{P}}+P_0}-V_{2\mathrm{P}}\frac{P_1}{K_{2\mathrm{P}}+P_1}-V_{3\mathrm{P}}\frac{P_1}{K_{3\mathrm{P}}+P_1}+V_{4\mathrm{P}}\frac{P_2}{K_{4\mathrm{P}}+P_2}-k_{\mathrm{d}}P_1$$

$$\frac{dP_2}{dt}=V_{3\mathrm{P}}\frac{P_1}{K_{3\mathrm{P}}+P_1}-V_{4\mathrm{P}}\frac{P_2}{K_{4\mathrm{P}}+P_2}-k_3P_2T_2+k_4C-v_{\mathrm{dP}}\frac{P_2}{K_{\mathrm{dP}}+P_2}-k_{\mathrm{d}}P_2$$

$$\frac{dM_T}{dt} = v_{sT}\frac{K_{IT}{}^n}{K_{IT}{}^n + C_N{}^n} - v_{mT}\frac{M_T}{K_{mT} + M_T} - k_d M_T$$
$$\frac{dT_0}{dt} = k_{sT}M_T - V_{1T}\frac{T_0}{K_{1T} + T_0} + V_{2T}\frac{T_1}{K_{2T} + T_1} - k_d T_0$$
$$\frac{dT_1}{dt} = V_{1T}\frac{T_0}{K_{1T} + T_0} - V_{2T}\frac{T_1}{K_{2T} + T_1} - V_{3T}\frac{T_1}{K_{3T} + T_1} + V_{4T}\frac{T_2}{K_{4T} + T_2} - k_d T_1$$
$$\frac{dT_2}{dt} = V_{3T}\frac{T_1}{K_{3T} + T_1} - V_{4T}\frac{T_2}{K_{4T} + T_2} - k_3 P_2 T_2 + k_4 C - v_{dT}\frac{T_2}{K_{dT} + T_2} - k_d T_2$$
$$\frac{dC}{dt} = k_3 P_2 T_2 - k_4 C - K_1 C + k_2 C_N - k_{dC} C$$
$$\frac{dC_N}{dt} = k_1 C - k_2 C_N - k_{dN} C_N$$

The total (nonconserved) quantities of PER and TIM proteins, P_t and T_t are given by

$$P_t = P_0 + P_1 + P_2 + C + C_N$$
$$T_t = T_0 + T_1 + T_2 + C + C_N$$

Table B1. Rate constants for the Drosophila model.

Kinetic parameter	Parameter value
v_{sP}	1 nM h^{-1}
v_{sT}	1 nM h^{-1}
v_{mP}	0.7 nM h^{-1}
v_{mT}	0.7 nM h^{-1}
K_{mP}	0.2 nM
K_{mT}	0.2 nM
k_{sP}	0.9 h^{-1}
k_{sT}	0.9 h^{-1}
v_{dP}	2 nM h^{-1}
v_{dT}	2 nM h^{-1}
k_1	0.6 h^{-1}
k_2	0.2 h^{-1}
k_3	1.2 nM^{-1} h^{-1}
k_4	0.6 h^{-1}
K_{IP}	1.0 nM
K_{IT}	1.0 nM
K_{dP}	0.2 nM
K_{dT}	0.2 nM
n	4
k_d	0.01 h^{-1}
k_{dC}	0.01 h^{-1}
k_{dN}	0.01 h^{-1}
V_{1P}	8 nM h^{-1}
V_{1T}	8 nM h^{-1}
V_{2P}	1 nM h^{-1}
V_{2T}	1 nM h^{-1}
V_{3P}	8 nM h^{-1}
V_{3T}	8 nM h^{-1}
V_{4P}	1 nM h^{-1}
V_{4T}	1 nM h^{-1}
K_{4T}	2.0 nM
K_{4P}	2.0 nM

(*continued*)

Table B1. (*Continued*).

Kinetic parameter	Parameter value
K_{3T}	2.0 nM
K_{3P}	2.0 nM
K_{2T}	2.0 nM
K_{2P}	2.0 nM
K_{1T}	2.0 nM
K_{1P}	2.0 nM